The rotational and fine-structure spectrum of FeH, studied by far-infrared laser magnetic resonance

John M. Brown[a)]
The Physical and Theoretical Chemistry Laboratory, Department of Chemistry, University of Oxford, South Parks Road, Oxford OX1 3QZ, United Kingdom

Helga Körsgen[b)]
Institut für Angewandte Physik, Universität Bonn, Wegelerstrasse 8, D53115 Bonn, Germany

Stuart P. Beaton[c)] and Kenneth M. Evenson[d)]
Time and Frequency Division, National Institute for Standards and Technology, Boulder, Colorado 80303

(Received 17 March 2006; accepted 31 March 2006; published online 20 June 2006)

Transitions between the spin-rotational levels of the FeH radical in the $v=0$ level of the $X\,^4\Delta$ ground state have been detected by the technique of laser magnetic resonance at far-infrared wavelengths. Both pure rotational and fine-structure transitions have been observed; lambda-type doubling is resolved on all the observed transitions. The energy levels of FeH are strongly affected by the breakdown of the Born-Oppenheimer approximation and cannot be modeled accurately by an effective Hamiltonian. The data are therefore fitted to an empirical formula to yield term values and g factors for the various spin-rotational levels involved. Many of the resonances show a doubling that arises from the proton hyperfine structure. These splittings are analyzed in a similar manner.
 [DOI: 10.1063/1.2198843]

I. INTRODUCTION

The FeH radical has been the object of curious enquiry for many years. There are two main reasons for this. First, it has the most complicated electronic structure of all the first-row transition metal monohydrides. Consequently, it presents a tough problem for both experimental and theoretical investigations; the two approaches help each other. From the experimental point of view, there is a need for detailed measurement and interpretation of spectroscopic observations to provide insight and benchmarks for *ab initio* calculations. Secondly, FeH is a molecule of considerable astronomical importance. The relatively high cosmic abundances of both ^{1}H (92.5%) and ^{56}Fe (0.003%)[1] suggest that the molecular species FeH is likely to be present in the atmospheres of stars and in the interstellar medium (ISM). FeH has indeed been detected in the atmospheres of the sun and other "cool" stars of spectral types M, S, and K.[2,3] In the last ten years, FeH has emerged as an important probe of the physical conditions of a new class of even cooler stars called brown dwarfs.[4,5] For this purpose, there is a pressing need for laboratory measurements of spectroscopic and magnetic properties of the molecule. At present, none of the several unassigned spectral lines due to molecules in the ISM has been assigned to transitions in FeH but it is hoped that, by providing accurate zero-field transition frequencies, the present study will help with these assignments in the far-infrared region.

FeH was probably first observed in the laboratory in the mid-1950s[6] when a band in the near infrared (NIR), at 989.6 nm, was attributed to FeH. In 1972, Carroll and McCormack[2] recorded two other band systems in the blue and the green regions of the visible spectrum that were also assigned to FeH. The lines that they reported accounted for some of the unassigned lines in the solar spectrum. In 1973, Klynning and Lindgren[7] recorded the NIR band at 989.6 nm at higher resolution. In 1976, Carroll *et al.*[3,8] published electronic spectra of FeH and FeD, which showed five band systems between 230 and 890 nm. The two most prominent of these systems were referred to as the green (530 nm) and blue (490 nm) systems. In all these studies, FeH was formed in a King furnace by passing H_2 over iron heated to about 2900 K.

In 1979, a study of FeH and FeD isolated in an argon matrix at a temperature of 4 K was published.[9] This work suggested vibrational wave numbers that differed from those determined by subsequent optical and infrared works; it has recently been shown that the species studied in these experiments were actually FeH_2 and FeD_2.[10] In 1983, a partial analysis of two of the NIR bands of FeD was reported.[11] In the same year, Stevens *et al.*[12] recorded the laser photoelectron spectra of FeH^- and FeD^-. A careful analysis of these results strongly suggested that the electronic ground state of FeH is $^4\Delta$ with a probable $^6\Delta$ state only 1945 cm^{-1} above it; these proposals have been confirmed subsequently. In 1987, Phillips *et al.*,[13] in a heroic piece of work, produced a detailed rotational analysis of the NIR bands of FeH.

In 1988, Beaton *et al.*[14] devised a method to form a sample of FeH radicals at near-ambient temperatures, using the gas-phase reaction between H atoms and $Fe(CO)_5$ vapor.

a)Author to whom correspondence should be addressed. Fax: (44)-1865-275410. Electronic mail: jmb@physchem.ox.ac.uk
b)Present address: Endress+Hauser BV, Nikkelstraat 6-12, NL-1411 AK Naarden, The Netherlands.
c)Present address: National Center for Atmospheric Research, Research Aviation Facility, 10802 Airport Court, Broomfield, CO 80021.
d)Deceased (29 January 2002).

In their paper, they reported the first observation of the far-infrared laser magnetic resonance (FIR LMR) spectrum of the FeH radical amongst others. The same production method was used by Towle *et al.*[15] to record the mid-infrared LMR spectrum of FeH in its ground $^4\Delta$ state and by Fletcher *et al.*[16] to record part of the green system in the electronic spectrum by laser excitation spectroscopy. The electronic spectrum, in particular, was considerably simplified compared with the high-temperature recordings made earlier; despite this, the rotational structure still defied analysis. The breakthrough in the analysis of the visible spectrum of FeH came with the observation and identification of the $g\,^6\Phi - X\,^4\Delta$ intercombination transition on the short-wavelength side of the blue system at 448 nm.[17,18] This led to the realization that the blue system of FeH was primarily attributable to the $g\,^6\Phi - a\,^6\Delta$ transition.[19] Indeed, it has emerged that most of the transitions in the blue and green systems of FeH start from the low-lying sextet states and not from the ground $^4\Delta$ state. By transferring knowledge of one state of FeH to another, the main transition in the green system was identified in 1996 as the $e\,^6\Pi - a\,^6\Delta$ transition.[20] Since then, many other features of the visible spectrum of FeH have been analyzed, including the identification of the $b\,^6\Pi$,[21] the $c\,^6\Sigma^-$,[22] and the $C\,^4\Phi$ states.[23] Further details of the spectrum have also been teased out[23–25] leading to the complete characterization of the $a\,^6\Delta$ state, that is, of all six spin components.[26] A further piece of the jigsaw puzzle that is the electronic spectrum of FeH has recently been filled in by Balfour *et al.* who have performed rotational analyses of the $E\,^4\Pi - X\,^4\Delta$ and $E\,^4\Pi - A\,^4\Pi$ transitions in the NIR;[27] this places the $A\,^4\Pi$ state just 970 cm^{-1} above the $X\,^4\Delta$ state.[28] As a result of all these works, FeH is now arguably the best characterized of all the first-row transition element hydrides.

These many experimental studies of FeH have been buttressed by a number of *ab initio* theoretical calculations. In the early days, the challenge was to determine the true identity of the ground electronic state of FeH. This was eventually achieved by Bauschlicher and Langhoff[29] in 1988 using a large Gaussian basis set and an extensive treatment of correlation and inner-shell correlation effects. The difficulty in the calculation arises largely because the configurations arising from the ground ^5D and low-lying excited ^5F states of atomic iron are very similar in energy and differ by a single spin-orbital.[30] Langhoff and Bauschlicher extended their CASSCF/MCRI calculation two years later to include all electronic states of quartet and sextet multiplicity below 25 000 cm^{-1}.[31] This second calculation has proved to be very reliable; indeed Langhoff and Bauschlicher were the first to suggest that the green and blue systems of FeH might draw their intensities primarily from the $e\,^6\Pi - a\,^6\Delta$ and $g\,^6\Phi - a\,^6\Delta$ transitions, respectively. The only limitation in the application of their calculations to the interpretation of spectroscopic data is that the effects of nonadiabatic mixing were not included. The state labels used in the present paper are taken from Langhoff and Bauschlicher's paper. The description of the electronic structure of FeH has been recognized as one of the most challenging of all diatomic molecules. Subsequent calculations have been used largely to test alternative theoretical approaches.[32,33]

The present paper is concerned with the observation and analysis of the pure rotational and fine-structure spectrum of FeH in the $v=0$ level of its $X\,^4\Delta$ state. These transitions fall in the far-infrared (FIR) region of the spectrum and have been recorded by LMR techniques. As such, it is the completion of the work started a long time ago by the first observation of the FIR LMR spectrum of FeH.[14] The end result is the precise measurement of term values for several rotational levels in all four spin components of the $X\,^4\Delta$ state. In addition, it has been possible to measure the magnetic properties and proton hyperfine splittings of the FeH molecule in these various rotational levels. It is demonstrated that FeH shows a drastic breakdown of the Born-Oppenheimer approximation in its ground $^4\Delta$ state.

II. EXPERIMENTAL DETAILS

The far-infrared LMR experiments were performed at the Boulder laboratories of NIST; the spectrometer has been described in detail elsewhere.[34] The FeH radicals were produced in the spectrometer sample volume by the reaction of hydrogen atoms with $Fe(CO)_5$ vapor in a flow system, the hydrogen atoms being generated by passing a mixture of 7.5% H_2 in helium through a microwave discharge. The total pressure in the sample volume ranged from 1.5 to 2.0 Torr (200–267 Pa); the partial pressure of $Fe(CO)_5$ was 0.15 Torr (20 Pa). Under these conditions, a black deposit of finely divided iron powder was put down in the reaction zone. The magnetic field was modulated at a frequency of 14 kHz and the signal was detected with a lock-in amplifier at the same frequency. The resonances were consequently displayed as the first derivative of an absorption profile. The magnet of the LMR system was controlled by a rotating-coil magnetometer which provided a direct readout of the flux densities. The system was calibrated periodically up to 1.8 T with a proton NMR gaussmeter; the absolute uncertainty was 10^{-5} T below 0.1 T and the fractional uncertainty was 10^{-4} above 0.1 T.

III. RESULTS AND ANALYSIS

A. Experimental observations

The first observation of the far-infrared LMR spectrum of FeH in the $v=0$ level was made using the 170.6 μm line of CH_3OH in March 1988.[14] The resultant spectrum is shown in Fig. 1. The spectrum was easily assigned to the rotational transition $J=5\frac{1}{2}-4\frac{1}{2}$ in the lowest, $\Omega=7/2$ spin component by use of the term values determined by Phillips *et al.*[13] from the electronic spectrum. The Zeeman patterns, consisting of the relative magnetic fields, relative intensities, and linewidths in milliteslas, in both π ($\Delta M_J=0$) and σ ($\Delta M_J=\pm 1$) polarizations are consistent with a linear Zeeman effect,

$$h\nu_L = h\nu_0 + (g'_J M'_J - g''_J M''_J)\mu_B B_Z. \quad (1)$$

In this equation, ν_L is the laser frequency, ν_0 is the zero-field transition frequency, g_J is the molecular g factor, and M_J is the quantum number for the component of the rotational angular momentum J along the direction of the magnetic flux

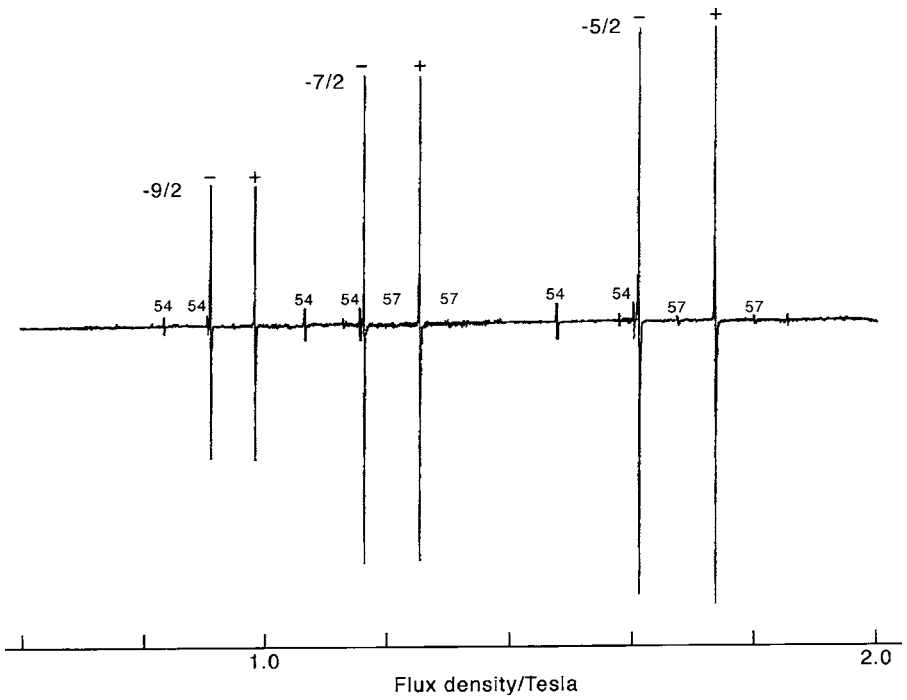

FIG. 1. Part of the far-infrared LMR spectrum of the FeH radical in the $v=0$ level of the $X\,^4\Delta$ state. The spectrum is recorded with the 170.6 μm laser line in parallel polarization ($\Delta M_J=0$). The pure rotational transition involved is $J=11/2\leftarrow 9/2$, $\Omega=7/2$; the values for the quantum number M_J are shown by the resonances. The very obvious doublet structure is caused by lambda-type doubling; the resonances are labeled by the parity of the lower state involved in the transition. The corresponding resonances for ^{54}FeH (5.8%) and even ^{57}FeH (2.2%) can also be identified.

B_Z; the single and double primes are used to distinguish the upper and lower levels involved in the transition, respectively. The large and obvious doublet structure on each resonance in Fig. 1 is attributable to lambda-type doubling. Further measurements of the LMR spectrum of FeH were made over the following few years. These resulted in the detection of many more rotational transitions, in all four spin components of the ground vibrational level. For reasons that will be explained later, it was desirable to record each transition with two or more laser lines. More recently, many new short-wavelength FIR laser lines have been discovered and frequency measured.[35–37] This provided the possibility of detecting several fine-structure transitions between adjacent spin components. An example, using the 43.7 μm line of CD_3OH is shown in Fig. 2; the transition involved is $J=5\frac{1}{2}-5\frac{1}{2}$, $\Omega=5/2-7/2$, $+\leftarrow-$. The identification of the fine-structure transitions was again straightforward with the help of the term values determined by Phillips *et al.*[13] that have proved to be very reliable. A summary of the various rotational and fine-structure transitions detected is given in Table I. They are also shown on the energy level diagram in Fig. 3. It can be seen that it has been possible to detect transitions in levels some 700 cm^{-1} above the lowest rotational level. The measurements of the individual resonances, together with their assignments, are available from the Electronic Physics Auxiliary Publication Service (EPAPS);[38] a small fraction of the data is given in Table II to show the information available. All the transitions detected, even the fine-structure transitions, are electric dipole in character and obey the parity selection rule, $+\leftrightarrow-$. Most of the resonances showed a small, doublet splitting attributable to the proton hyperfine structure; an example of such hyperfine structure from the

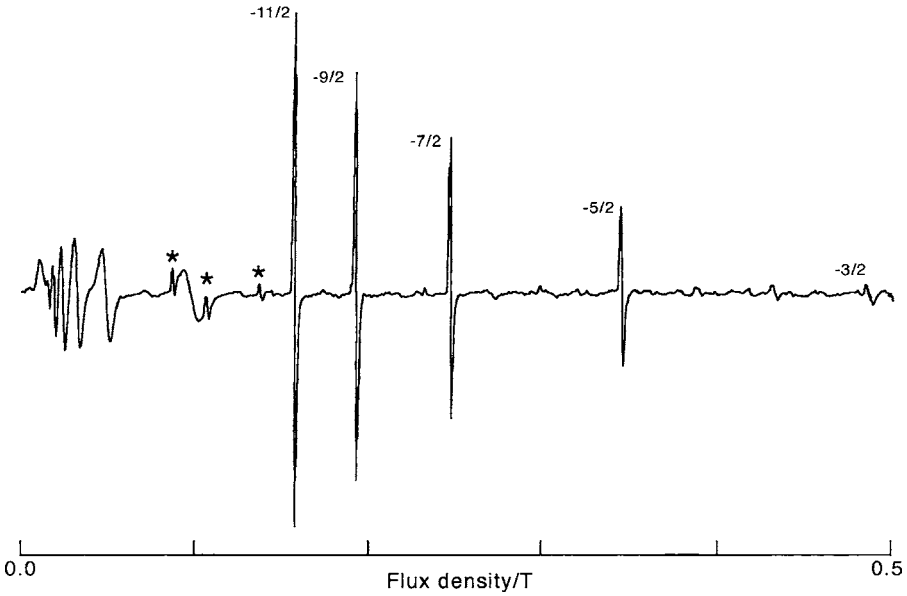

FIG. 2. Part of the far-infrared LMR spectrum of the ^{56}FeH radical in the $v=0$ level of the $X\,^4\Delta$ state, recorded with the 43.70 μm laser line in parallel polarization ($\Delta M_J=0$). The transition involved in the main Zeeman progression is an electric-dipole fine-structure transition, $\Omega=5/2\leftarrow 7/2$, $J=11/2\leftarrow 11/2$, $-\leftarrow+$; the values for M_J involved are shown by the resonances. The corresponding resonances for ^{54}FeH can be seen at lower flux densities (marked with asterisks). The Zeeman progression at very low fields has not yet been assigned; the relative intensities of successive resonances indicate that the transition obeys the selection rule $\Delta J=\pm 1$.

TABLE I. Summary of observations in the far-infrared LMR spectrum of FeH in its $X\,^4\Delta$ state.

FeH transitions observed			Laser line			
Ω	J	Parity	$\lambda(\mu m)$	ν(GHz)	Gas	Pump
			Rotational transitions			
7/2	9/2–7/2	$\mp\leftarrow\pm$	214.6	1397.11186	CH_2F_2	$9R(34)$
			211.3	1419.0493	CH_3OH	$10R(4)$
	11/2–9/2	$\pm\leftarrow\mp$	171.8	1745.4390	$^{13}CH_3OH$	$10R(18)$
			170.6	1757.5263	CH_3OH	$9P(36)$
	13/2–11/2	$\mp\leftarrow\pm$	144.1	2080.1893	CD_3OH	$10P(18)$
	15/2–13/2	$\pm\leftarrow\mp$	122.5	2447.9685	CH_2F_2	$9R(22)$
5/2	7/2–5/2	$\pm\leftarrow\mp$	227.7	1316.8387	CD_3OD	$10R(10)$
			226.3	1324.7719	CH_2DOH	$9P(46)$
	11/2–9/2	$+\leftarrow-$	144.1	2080.1893	CD_3OH	$10P(18)$
	13/2–11/2	$-\leftarrow+$	122.5	2447.9685	CH_2F_2	$9R(22)$
3/2	5/2–3/2	$-\leftarrow+$	286.2	1047.6576	CH_3OH	$10R(48)$
			280.9	1067.1272	CH_3OH	$9R(18)$
		$+\leftarrow-$	293.8	1020.3211	CH_3OH	$10R(10)$
			290.7	1031.3844	CD_3OD	$10R(14)$
1/2	3/2–1/2	$+\leftarrow-$	410.7	729.9328	CD_3OD	$10R(12)$
			407.3	736.0596	CH_2CF_2	$10P(14)$
	5/2–3/2	$+\leftarrow-$	272.3	1100.8067	CH_2F_2	$9P(10)$
			Fine-structure transitions			
5/2–7/2	7/2–9/2	$\pm\leftarrow\mp$	62.50	4796.7516	$^{13}CD_3OH$	$10R(8)$
	9/2–11/2	$\mp\leftarrow\pm$	62.50	4796.7516	$^{13}CD_3OH$	$10R(8)$
			63.10	4751.3418	$^{13}CH_3OH$	$9P(12)$
			63.37	4730.8606	CH_3OH	$9P(34)$
	11/2–13/2	$\pm\leftarrow\mp$	63.10	4751.3418	$^{13}CH_3OH$	$9P(12)$
			63.37	4730.8606	CH_3OH	$9P(34)$
	13/2–15/2	$\mp\leftarrow\pm$	63.10	4751.3418	$^{13}CH_3OH$	$9P(12)$
			63.37	4730.8606	CH_3OH	$9P(34)$
	7/2–7/2	$\pm\leftarrow\mp$	48.28	6209.0872	CH_3OH	$10R(32)$
	9/2–9/2	$\mp\leftarrow\pm$	46.17	6493.9115	CH_3OH	$9P(10)$
	11/2–11/2	$\pm\leftarrow\mp$	43.70	6860.6642	CD_3OH	$10R(18)$
			43.78	6847.4732	CH_3OH	$10R(36)$
	13/2–13/2	$-\leftarrow+$	41.36	7249.2660	CD_3OH	$10R(18)$
		$+\leftarrow-$	41.87	7159.8953	CH_3OH	$9P(16)$
	15/2–15/2	$-\leftarrow+$	39.92	7509.0362	CH_3OH	$9P(34)$
3/2–5/2	3/2–5/2	$\pm\leftarrow\mp$	48.28	6209.0872	CH_3OH	$10R(32)$
			48.72	6153.2790	CD_3OH	$9R(6)$
	5/2–5/2	$-\leftarrow+$	41.36	7249.2660	CD_3OH	$10R(18)$

170.6 μm spectrum is shown in Fig. 4. These hyperfine splittings (in milliteslas) are also listed in Table II. The vast majority of the observations refer to the dominant isotopomer, ^{56}FeH; these were the only transitions that were searched for deliberately. However, it was also often possible to detect signals for the ^{54}FeH (5.8%) and ^{57}FeH (2.2%) isotopomers in natural abundance. Such signals are clearly visible in Figs. 1, 2, and 4.

B. Analysis of the data

In the past, we have enjoyed considerable success in analyzing LMR spectra of open-shell molecules in terms of an effective Hamiltonian.[39,40] This is an operator that describes the rotational energy levels of a molecule, including fine and hyperfine structures, in a particular vibrational level of a single electronic state in terms of molecular parameters.[41,42] These parameters, such as the rotational constant B or the spin-spin coupling constant λ, absorb the effects of mixing of adjacent vibrational and electronic states. Explicit formulas for the parameters can be obtained by some chosen perturbative procedure.[41] The success of the effective Hamiltonian approach thus depends on the off-diagonal mixing effects being much smaller than the separation between the various vibrational and electronic states. This is not the case in FeH. Six electronic states have been identified within 5000 cm^{-1} of the ground $^4\Delta$ state; the $A\,^4\Pi$ state lies only 970 cm^{-1} above the $X\,^4\Delta$ state,[27] closer even than the first vibrational level at 1759 cm^{-1}.[15] FeH is therefore a molecule for which the Born-Oppenheimer approximation fails catastrophically and the effective Hamiltonian simply does not work. The best attempt to fit a Hamiltonian with a large number (13) of parameters to the term values of

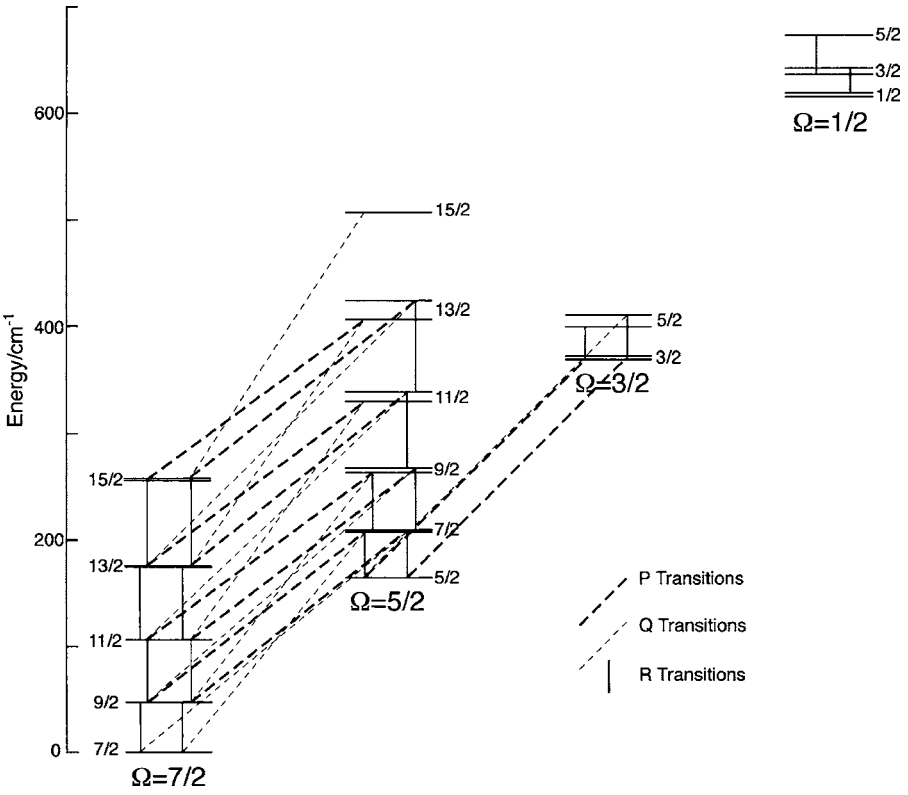

FIG. 3. Diagram showing the lower energy levels of the FeH radical in the $v=0$ level of the $X\,^4\Delta$ state and the transitions involved in the observed far-infrared LMR spectrum. The lambda-type (parity) doubling has been exaggerated by a factor of 10 for the sake of clarity. It can be seen that the fine-structure transitions occur at much shorter wavelengths than the pure rotational transitions.

the $v=0$ level of the $X\,^4\Delta$ state has a standard deviation of fit of a few cm^{-1}, almost a thousand times larger than the experimental precision of measurement.

These characteristics of FeH have forced us to adopt a more phenomenological approach to the analysis of its far-infrared LMR spectra. We describe each individual spin-rotational energy level by the formula

$$E_{J,\Omega,\mathrm{par}}(M_J) = E_0 + g_J\mu_B B_Z M_J + c_1\mu_B^2 B_Z^2 + c_2\mu_B^2 B_Z^2 M_J^2, \tag{2}$$

where E_0 is the zero-field energy of a level characterized by its J, Ω, and parity values. The second term on the right hand side describes the dominant linear Zeeman effect in terms of Landé-type g factor. The third and fourth terms on the right hand side model the second-order Zeeman effect arising from the admixture of adjacent rotational levels; these terms are expected to be smaller than the linear effect. The formula given in Eq. (2) can be regarded as an extension of that given in Eq. (1).

Consider the case where we record the LMR spectrum for a single rotational transition with a particular laser line in both parallel ($\Delta M_J=0$) and perpendicular ($\Delta M_J=\pm 1$) polarizations. This provides two independent pieces of experimental information. When we try to describe these two spectra with Eq. (1), we see that there are three unknowns, $(\nu_L - \nu_0)$, g_J', and g_J''. Thus it is not possible to determine all three of these parameters from the LMR observation with a single laser line. For this reason, we have attempted to record the LMR spectra associated with each rotational transition on at least two different laser lines. It can be seen from Table I that this has not always been possible. However, if information on the Zeeman parameters of one of the two levels involved is available from the spectrum of a different transition, it is still possible to include a single laser observation in the global fit.

We have carried out a global fit of all the LMR data for the three lowest spin components ($\Omega=7/2$, $5/2$, and $3/2$) by linear least squares to determine values for the parameters E_0, g_J, c_1, and c_2 in Eq. (2) for each rotational level involved; the lowest rotational level ($J=7/2$, $\Omega=7/2$, and parity$=-$) was taken as the zero of energy in the fit. It has not been possible to include the observations on the highest spin component ($\Omega=1/2$) because we have not detected any fine-structure transitions that connect it to the lower spin components. Each data point in the fit was assigned the same weight, consistent with an experimental uncertainty of measurement of 2 MHz. A few resonances in the spectrum for the 144.1 μm line had very large residuals and so were excluded from the final fit of 352 data points. These large residuals almost certainly arise from experimental mismeasurements; unfortunately, it has not been possible to repeat them. The standard deviation of the fit relative to experimental uncertainty was 0.879, an entirely satisfactory result. The values for the various parameters determined are listed in Table III, together with their estimated uncertainties. The residuals from this fit are given in Table II.[38]

The LMR spectrum associated with the $J=3/2\leftarrow 1/2$, $+\leftarrow -$ transition in the $\Omega=\frac{1}{2}$ spin component has been recorded on two laser lines but is unfortunately not connected with the rest of the data set. The measurements are well described by a linear Zeeman effect, Eq. (1). The data and the results of the fit are given in Table IV. Note that the signs of the g factors are not determinable from these observations. The data can be fitted equally well by changing the signs of the M_J quantum numbers throughout.

TABLE II. A small part of the observations and assignments in the far-infrared LMR spectrum of the FeH radical in the $v=0$ level of the $X\,^4\Delta$ state. A complete version of this table is available as supplementary material Ref. 38.

$J' \leftarrow J''$	$\Omega' \leftarrow \Omega''$	Parity	$M'_J \leftarrow M''_J$	ν_L (MHz)	B_0 (mT)	ΔB[a] (mT)	$\nu_L - \nu_{calc}$ (MHz)	$\partial\nu/\partial B_0$ (MHz/mT)
9/2←7/2	7/2	+←−	7/2←7/2	1 397 118.6	825.52	0.680	−0.5	−16.94
		−←+	7/2←7/2		840.74	0.691	−2.4	−16.95
		+←−	5/2←5/2		1166.44	0.716	0.7	−11.88
		−←+	5/2←5/2		1188.05	0.718	0.3	−11.89
		+←−	5/2←7/2		472.68	[b]	−0.9	−29.58
		−←+	5/2←7/2		481.55	[b]	−2.0	−29.58
		+←−	3/2←5/2		566.36	[b]	−0.9	−24.63
		−←+	3/2←5/2		577.02	[b]	−2.0	−24.63
		+←−	1/2←3/2		706.54	[b]	−0.2	−19.67
		−←+	1/2←3/2		719.93	[b]	−0.6	−19.67
		+←−	−1/2←1/2		939.27	[b]	−2.1	−14.70
		−←+	−1/2←1/2		957.36	[b]	−0.2	−14.70
		+←−	−3/2←−1/2		1404.47	[b]	1.8	−9.68
		−←+	−3/2←−1/2		1431.23	[b]	−3.2	−9.68
9/2←7/2	7/2	−←+	−7/2←−7/2	1 419 049.3	454.78	[b]	2.8	16.90
		+←−	−7/2←−7/2		470.69	[b]	2.6	16.89
		−←+	−5/2←−5/2		633.69	0.724	1.9	12.19
		+←−	−5/2←−5/2		655.71	0.714	1.3	12.19
		−←+	−3/2←−3/2		1038.58	[b]	−0.1	7.56
		+←−	−3/2←−3/2		1073.99	[b]	−3.1	7.58
		−←+	−3/2←−5/2		310.87	[b]	0.9	24.76
		+←−	−3/2←−5/2		321.59	[b]	1.1	24.76
		−←+	−1/2←−3/2		385.69	[b]	1.0	20.00
		+←−	−1/2←−3/2		398.96	[b]	0.5	20.00
		−←+	1/2←−1/2		507.88	[b]	0.3	15.24
		+←−	1/2←−1/2		525.16	[b]	0.2	15.25
		−←+	3/2←1/2		742.61	0.529	0.3	10.50
		+←−	3/2←1/2		767.46	0.550	−0.4	10.52
		−←+	5/2←3/2		1373.06	1.516	0.4	5.82
		+←−	5/2←3/2		1416.76	1.534	−2.4	5.85

[a]ΔB is the proton hyperfine splitting observed on a resonance (in mT).
[b]H hyperfine splitting not resolved.

C. Analysis of the proton hyperfine structure

The majority of the resonances observed show a small doublet splitting that is attributable to the proton $\left(I=\frac{1}{2}\right)$ hyperfine interaction. This splitting arises from the coupling between the nuclear spin magnetic moment and the magnetic moments caused by the electron spin and orbital motions and by the rotational motion of the molecule as a whole. At least five independent parameters are required to describe these various interactions in the effective Hamiltonian.[42] Such a treatment cannot be applied in this case since the effective Hamiltonian is not even capable of describing the spin-rotational levels of FeH in its ground $^4\Delta$ state. We have therefore fitted the observed splittings to the phenomenonological Hamiltonian[43]

$$H_{\rm hfs} = A_{\rm hfs}\mathbf{I}\cdot\mathbf{J}, \tag{3}$$

where $A_{\rm hfs}$ is a parameter that has a different value for each individual rotational level of given parity. Because the hyper-

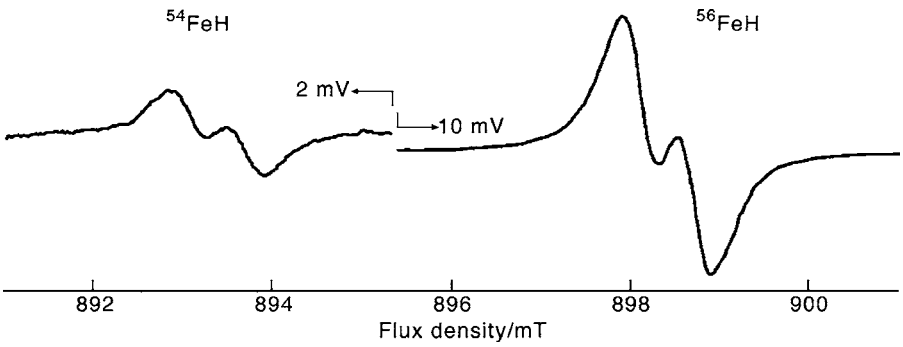

FIG. 4. A small portion of the FIR LMR spectrum of the FeH radical in the $v=0$ level of the $X\,^4\Delta$ state, recorded with the 170.6 μm laser line in parallel polarization ($\Delta M_J=0$); the complete spectrum is shown in Fig. 1. The partially resolved doublet structure on each resonance is caused by the proton hyperfine interaction. The lower field resonance is assigned to ^{54}FeH (5.8%) and the higher field resonance to ^{56}FeH (91.7%). Note the change of amplifier sensitivity between the two parts of the scan.

TABLE III. Values for parameters determined in the least-squares fit of far-infrared LMR data for FeH in the $v=0$ level of the $X\,^4\Delta$ state.

Ω	J	Parity	E(GHz)	g_J	$10^3\,c_1$ (GHz^{-1})	$10^4\,c_2$ (GHz^{-1})
7/2	7/2	−	0.00000[a]	1.248 023(37)[b]	0.0[c]	0.9899(71)
		+	0.049 4(20)	1.247 946(32)	0.0076(59)	0.9791(63)
	9/2	+	1 411.092 41(68)	0.902 844(29)	0.9841(40)	0.0984(47)
		−	1 411.407 2(19)	0.902 630(23)	0.9725(50)	0.1037(38)
	11/2	−	3 156.891 77(82)	0.711 096(29)	1.2537(44)	−0.0070(29)
		+	3 158.055 8(19)	0.710 532(22)	1.2287(54)	0.0033(25)
	13/2	+	5 245.275 7(27)	0.591 091(39)	1.3205(61)	−0.0087(41)
		−	5 248.433 2(26)	0.590 154(76)	1.2936(65)	−0.0002(51)
	15/2	−	7 683.069 4(41)	0.509 540(92)	1.331(13)	0.0062(78)
		+	7 690.101 9(35)	0.507 909(74)	1.2927(69)	0.0103(48)
5/2	5/2	+	4 915.247 8(27)	1.132 507(66)	0.4122(75)	1.336(17)
		−	4 915.967 8(24)	1.131 387(39)	0.4082(63)	1.363(17)
	7/2	−	6 236.094 3(26)	0.686 094(50)	1.5418(66)	−0.2212(88)
		+	6 240.067 6(23)	0.682 869(52)	1.5007(50)	−0.1823(89)
	9/2	+	7 926.927 5(15)	0.485 076(37)	1.7713(52)	−0.2041(42)
		−	7 939.346 6(22)	0.478 637(45)	1.6416(64)	−0.1377(50)
	11/2	−	9 984.491 5(27)	0.377 72(42)	1.8329(60)	−0.1361(38)
		+	10 013.444 96(93)	0.367 862(30)	1.6129(58)	−0.0569(51)
	13/2	+	12 406.554 3(32)	0.313 726(58)	1.859(14)	−0.0859(48)
		−	12 462.653 7(10)	0.300 456(29)	1.5331(63)	−0.0123(24)
	15/2	−	15 192.094(17)	0.270 4(12)	2.023(79)	−0.38(26)
3/2	3/2	−	11 089.580 9(51)	0.793 974(66)	1.262(12)	1.160(40)
		+	11 098.931 4(34)	0.772 144(63)	1.1295(81)	1.441(31)
	5/2	+	12 118.450 2(51)	0.344 630(65)	2.078(14)	−0.736(19)
		−	12 153.361 1(31)	0.311 283(45)	1.8003(96)	−0.391(15)

[a]The energy levels are measured relative to the lower lambda doublet (−parity) of the $J=7/2$ level of the $\Omega=7/2$ spin component.
[b]The figures in parentheses are the standard deviations determined in the least-squares fit, in units of the last quoted decimal place.
[c]The value for the parameter c_1 for the base level is not determinable and is assumed to be zero.

fine splittings are small and the resonances are all observed at fields greater than 50 mT, it is justifiable to describe the nuclear spin state as decoupled, $|I,M_I\rangle$. The energy of an individual nuclear spin state under these conditions is therefore

$$E_{\rm hfs} = A_{\rm hfs} M_J M_I. \tag{4}$$

For $I=\frac{1}{2}$, the observed splitting is the difference of the splittings in the upper and lower levels:

$$\Delta\nu_{\rm hfs} = A^{\pm}_{\rm hfs}(J',\Omega')M'_J - A^{\mp}_{\rm hfs}(J'',\Omega'')M''_J. \tag{5}$$

The observed splittings in milliteslas were converted to splittings in megahertz by use of the tuning rates given in Table II.[38] All of the observed hyperfine splittings were adequately fitted by this model. The parameters $A_{\pm}$ were assumed to be positive; the values determined are given in Table V. In the absence of a magnetic field, each rotational level is split into two closely spaced levels with $F=J+\frac{1}{2}$ and $F=J-\frac{1}{2}$. The

TABLE IV. Details of the far-infrared LMR spectra recorded for the $J=3/2\leftarrow 1/2$, $+\leftarrow -$ transition in the $\Omega=\frac{1}{2}$ spin component of the FeH radical in the $v=0$ level of the $X\,^4\Delta$ state. Results of least-squares fit: $\nu_0=730\,914.80(4)$ MHz, $g'_J=-0.280\,423(59)$, and $g''_J=-0.525\,071(89)$.

$J'\leftarrow J''$	$\Omega'\leftarrow\Omega''$	Parity	$M'_J\leftarrow M''_J$	ν_L (MHz)	B_0 (mT)	ΔB[a] (mT)	$\nu_L-\nu_{\rm calc}$ (MHz)	$\partial\nu/\partial B_0$ (MHz/mT)
$3/2\leftarrow 1/2$	1/2	$+\leftarrow -$	$-1/2\leftarrow -1/2$	729 932.8	573.60	5.70	0.03	−1.71
		$+\leftarrow -$	$1/2\leftarrow -1/2$		174.20	4.03	−0.06	−5.63
		$+\leftarrow -$	$3/2\leftarrow 1/2$		443.80	[b]	0.02	−2.21
		$+\leftarrow -$	$-1/2\leftarrow 1/2$	736 059.6	912.69	3.87	0.00	5.63

[a]ΔB is the proton hyperfine splitting observed on a resonance (in mT).
[b]H hyperfine splitting not resolved.

TABLE V. Values for the proton hyperfine parameters for rotational levels of FeH in the v=0 level of the $X\,^4\Delta$ state.

Ω	J	Parity	$A^{\pm}_{\rm hfs}$ (MHz)	Splitting (MHz)[a]
7/2	7/2	−	11.93(72)	47.72
		+	13.4(12)	53.6
	9/2	+	8.26(57)	41.30
		−	9.54(96)	47.70
	11/2	−	6.42(49)	38.52
		+	7.76(86)	46.56
	13/2	+	7.31(59)	51.17
		−	6.84(47)	47.88
	15/2	−	6.57(81)	52.56
		+	7.41(58)	59.28
5/2	9/2	+	2.45(61)	12.25
		−	4.2(11)	21.0
	11/2	−	3.32(67)	19.92
		+	2.54(53)	15.24
	13/2	+	2.30(90)	16.10
		−	2.99(63)	20.93
3/2	3/2	−	5.4(18)	10.8
		+	5.7(18)	11.4
	5/2	−	4.0(40)	12.0
		+	3.5(40)	10.5

[a]This is the calculated value for the zero-field hyperfine splitting of the rotational level in question. Note that the relative order of the two hyperfine levels is not determined by the present experiments.

diagonal matrix element of $H_{\rm hfs}$ in an I-coupled basis set (appropriate to the zero-field situation) is

$$E_{\rm hfs} = \tfrac{1}{2}A_{\rm hfs}[F(F+1) - J(J+1) - I(I+1)]. \quad (6)$$

The zero-field hyperfine splittings calculated with this formula are equal to $\frac{1}{2}A_{\rm hfs}(2J+1)$; they are also given in Table V. We emphasize that the relative order of the two hyperfine components is not determined by our observations.

IV. DISCUSSION

In this paper, we report the observation of many rotational and fine-structure transitions between low-lying levels of FeH in its $X\,^4\Delta$ state by FIR LMR. These measurements have been fitted with a phenomenological model to determine a set of energy levels and Zeeman parameters for 25 individual levels of FeH. The present results are consistent with but more accurate than the previous measurements of these term values by Phillips *et al.*[13] from the electronic spectrum, see Table VI. Nevertheless, the table bears witness to the accuracy of the optical term values for the v=0 level (0.01 $\rm cm^{-1}$). We can use the results to predict the pure rotational transition frequencies of FeH in the Ω=7/2 component that are most likely to be detected in the interstellar medium:

$J = 9/2 \leftarrow 7/2, \quad + \leftarrow -,$

$\nu = 1\,411\,092.41(68)$ MHz,

hyperfine splitting ≅ 6.4 MHz,

$J = 9/2 \leftarrow 7/2, \quad - \leftarrow +,$

$\nu = 1\,411\,357.8(28)$ MHz,

hyperfine splitting ≅ 5.9 MHz,

$J = 11/2 \leftarrow 9/2, \quad - \leftarrow +,$

$\nu = 1\,745\,799.4(11)$ MHz,

hyperfine splitting ≅ 2.8 MHz,

$J = 11/2 \leftarrow 9/2, \quad + \leftarrow -,$

$\nu = 1\,746\,648.6(28)$ MHz,

hyperfine splitting ≅ 1.1 MHz.

In addition to the term values, we have determined Landé-type g factors for the individual rotational levels studied. Reference to Table III shows that the values obtained decrease with increasing J values and with decreasing Ω values. Such behavior is broadly in line with expectation for a Hund's case (a) coupling scheme:[42]

$$g_J = (g_S\Sigma + g_L\Lambda)\Omega/[J(J+1)]. \quad (7)$$

The two major contributions to the molecular magnetic moment of an open-shell molecule are from the electron orbital and electron spin angular momenta:

$$H_{\rm Zeemon} = g_L\mu_B L_Z B_Z + g_S\mu_B S_Z B_Z + \text{smaller terms}. \quad (8)$$

If one works out the matrix elements of this operator in a Hund's case (a) basis set and treats the matrix elements diagonal in J but off diagonal in Ω by second-order perturbation theory, the g_J factors are given by the following expressions in the four components of the $^4\Delta$ state:

$$\Omega = 7/2, \quad g_J = \frac{\left(2g_L + \frac{3}{2}g_S\right)\frac{7}{2}}{J(J+1)} - \frac{3(z-9)B^* g_S^*}{J(J+1)(E_1 - E_2)}, \quad (9)$$

$$\Omega = 5/2, \quad g_J = \frac{\left(2g_L + \frac{1}{2}g_S\right)\frac{5}{2}}{J(J+1)} + \frac{3(z-9)B^* g_S^*}{J(J+1)(E_1 - E_2)} - \frac{4(z-4)B^* g_S^*}{J(J+1)(E_2 - E_3)}, \quad (10)$$

$$\Omega = 3/2, \quad g_J = \frac{\left(2g_L - \frac{1}{2}g_S\right)\frac{3}{2}}{J(J+1)} + \frac{4(z-4)B^* g_S^*}{J(J+1)(E_2 - E_3)} - \frac{3(z-1)B^* g_S^*}{J(J+1)(E_3 - E_4)}, \quad (11)$$

$$\Omega = 1/2, \quad g_J = \frac{\left(2g_L - \frac{3}{2}g_S\right)\frac{1}{2}}{J(J+1)} + \frac{3(z-1)B^* g_S^*}{J(J+1)(E_3 - E_4)}, \quad (12)$$

where $z \equiv (J+\frac{1}{2})^2$, $B^* = B - \frac{1}{2}\gamma$, $g_s^* = g_s + g_l$, and E_1, E_2, E_3, and E_4 are the energies of the four spin components in order of increasing energy. These formulas reproduce the experimental g_J factors only moderately well as is shown in Table VII, better for the lower spin components than the higher ones.

TABLE VI. Term values for rotational levels of FeH in the $v=0$ levels of the $X\,^4\Delta$ state, determined by far-infrared LMR.

Ω	J	Parity	E (GHz)	T (cm^{-1})	Phillips *et al.* (Ref. 13)
7/2	7/2	−	0.000 00[a]	0.000 00[a]	0.00
		+	0.049 4(20)[b]	0.001 648(67)	0.00
	9/2	+	1 411.092 41(68)	47.068 976(23)	47.07
		−	1 411.407 2(19)	47.079 477(63)	47.08
	11/2	−	3 156.891 77(82)	105.302 575(27)	105.32
		+	3 158.055 8(19)	105.341 403(87)	105.32
	13/2	+	5 245.275 7(27)	174.963 56(14)	174.96
		−	5 248.433 2(26)	175.068 887(87)	175.07
	15/2	−	7 683.069 4(41)	256.279 61(14)	256.27
		+	7 690.101 9(35)	256.514 19(12)	256.50
5/2	5/2	+	4 915 247 8(27)	163.955 019 2(90)	163.98
		−	4 915.967 8(24)	163.979 035(80)	163.98
	7/2	−	6 236.094 3(26)	208.013 715(87)	208.01
		+	6 240.067 6(23)	208.146 250(77)	208.12
	9/2	+	7 926.927 5(15)	264.413 840(50)	264.40
		−	7 939.346 6(22)	264.828 097(73)	264.82
	11/2	−	9 984.491 5(27)	333.046 787(90)	333.04
		+	10 013.444 96(93)	334.012 571(31)	334.00
	13/2	+	12 406.554 3(32)	413.838 11(11)	413.83
		−	12 462.653 7(10)	415.709 381(33)	415.71
	15/2	−	15 192.094(17)	506.753 71(57)	506.75
3/2	3/2	−	11 089.580 9(51)	369.908 60(17)	369.90
		+	11 098.931 4(34)	370.220 50(11)	370.22
	5/2	+	12 118.450 2(51)	404.227 99(17)	404.19
		−	12 153.361 1(31)	405.392 49(10)	405.52

[a]The energy levels are measured relative to the lower lambda doublet (-parity) of the $J=7/2$ levels of the $\Omega=7/2$ spin component.
[b]The figures in parentheses are one standard deviation of the least-squares fit, in units of the last quoted decimal place.

The g factors used in these calculations have been determined in a least-squares fit of the experimental g_J factors to this model.[44] Our inability to fit the experimental data in this way is further evidence of the breakdown of the Born-Oppenheimer approximation for FeH; the Zeeman parameters are particularly sensitive to the mixing with nearby electronic states. Turning the argument the other way around, accurate measurements of the g factors provide direct information on the electronic structure of the molecule. Knowledge of the g factors is also important for astrophysicists who are studying the newly recognized class of cool substellar objects known as brown dwarfs. The $F\,^4\Delta - X\,^4\Delta$ transition of FeH is a dominant feature in the near-infrared spectra of these dwarfs[4,5] and has the potential to provide important information about the surface conditions, including the local magnetic fields (magnetic fields are thought to play an important role in the formation of such objects). Both these reasons emphasize the importance of making laboratory measurements of the Zeeman effect on FeH.

Although the present paper reports extensive measurements on FeH in its ground state by FIR LMR, much remains to be done in this spectral region. In particular, it is important to obtain more information on FeH in the highest, $\Omega=1/2$ component. These levels are difficult to study by LMR methods because they are relatively insensitive to magnetic fields and are not well populated at ambient tempera-

TABLE VII. Comparison of the experimentally determined g_J values for FeH in the $v=0$ level of the $X\,^4\Delta$ state with the values calculated from a Hund's case (a) formula.

Ω	J	$g_J^{(1)a}$	$g_J^{(2)b}$	g_J (Calc.)[c]	g_J (Expt.)[d]
7/2	7/2	1.1339	0.1278	1.2617	1.247 985(35)
	9/2	0.7216	0.1860	0.9076	0.902 737(26)
	11/2	0.4995	0.2173	0.7168	0.710 814(26)
	13/2	0.3663	0.2326	0.6023	0.590 623(58)
	15/2	0.2801	0.2482	0.5283	0.508 725(83)
5/2	5/2	0.9701	0.1783	1.1484	1222 947(69)
	7/2	0.5390	0.1099	0.6489	0.684 482(51)
	9/2	0.3430	0.0788	0.4218	0.481 857(41)
	11/2	0.2374	0.0621	0.2995	0.372 79(42)
	13/2	0.1741	0.0520	0.2661	0.307 091(44)
	15/2	0.1332	0.0455	0.1787	[0.270 4(12)][e]
3/2	3/2	0.6754	0.1637	0.8391	0.783 059(65)
	5/2	0.2895	0.0088	0.2983	0.327 957(55)

[a]First-order contribution to the g_J factor from Eqs. (9)–(12), using $g_s=1.707$ and $g_L=1.271$ (Ref. 44).
[b]Second-order contribution to the g_J factor from Eqs. (9)–(12), using $B=6.4848\ cm^{-1}$, $\gamma=-5.464\ cm^{-1}$, $g_l=0.281$, $(E_1-E_2)=-191.09\ cm^{-1}$, $(E_2-E_3)=-234.85\ cm^{-1}$, and $(E_3-E_4)=-268.62\ cm^{-1}$ (Ref. 44).
[c]Total calculated g_J factor, the sum of the first- and second-order contributions.
[d]The experimental values are the average values of the two lambda doublets, given in Table III.
[e]The experimental value is that for the − parity lambda doublet.

tures. They can, however, be accessed most easily by fine-structure transitions from the $\Omega=3/2$ component in the 40 μm region. It would also be very worthwhile to make an analogous study of the FeD isotopomer. The rotational analysis of the $F\,^4\Delta-X\,^4\Delta$ (Ref. 13) transition of this species,[11] although ground breaking, was not as thorough as that of FeH and, in particular, the spin-orbit splittings were not determined. A knowledge of these fine-structure intervals is important for the understanding of the electronic structure of FeH.

ACKNOWLEDGMENTS

The authors are very grateful to Ségolène Laage for her help with the final fits of the term values and of the hyperfine splittings. One of the authors (S.P.B.) is an employee of the National Center for Atmospheric Research which is funded by the National Science Foundation. The study of the LMR spectrum of FeH was supported in part by NASA Contract No. W15,047.

[1] M. Rowan-Robinson, *Cosmology* (Clarendon, Oxford, 1981).
[2] P. K. Carroll and P. McCormack, Astrophys J. Lett. **177**, L33 (1972).
[3] P. K. Carroll, P. McCormack, and S. O'Connor, Astrophys. J. **208**, 903 (1976).
[4] J. D. Kirkpatrick, I. N. Reid, J. Liebert, R. M. Cutri, B. Nelson, C. A. Biechman, C. C. Dahn, D. G. Monet, J. E. Gizis, and M. F. Skrutskie, Astrophys. J. **519**, 802 (1999).
[5] J. D. Kirkpatrick, F. Allard, T. Bida, B. Zuckerman, E. E. Becklin, G. Chabrier, and I. Baraffe, Astrophys. J. **519**, 834 (1999).
[6] B. Kleman and L. Åkerlind (unpublished work, 1958), see Ref. 7.
[7] L. Klynning and B. Lindgren, University of Stockholm USIP Report No. 73-20, 1973 (unpublished).
[8] P. K. Carroll, P. McCormack, and S. O'Connor, Astron. Astrophys., Suppl. Ser. **26**, 373 (1976).
[9] A. Dendramis, R. J. Van Zee, and W. Weltner, Jr., Astrophys. J. **231**, 632 (1979).
[10] H. Körsgen, W. Urban, and J. M. Brown, J. Chem. Phys. **110**, 3861 (1999).
[11] W. J. Balfour, B. Lindgren, and S. O'Connor, Phys. Scr. **28**, 551 (1983).
[12] A. E. Stevens, C. S. Feigerle, and W. C. Lineberger, J. Chem. Phys. **78**, 5420 (1983).
[13] J. G. Phillips, S. P. Davis, B. Lindgren, and W. J. Balfour, Astrophys. J. Suppl. **65**, 721 (1987).
[14] S. P. Beaton, K. M. Evenson, T. Nelis, and J. M. Brown, J. Chem. Phys. **89**, 4446 (1988).
[15] J. P. Towle, J. M. Brown, K. Lipus, E. Bachem, and W. Urban, Mol. Phys. **79**, 835 (1993).
[16] D. A. Fletcher, R. T. Carter, J. M. Brown, and T. C. Steimle, J. Chem. Phys. **93**, 9192 (1990).
[17] R. T. Carter, T. C. Steimle, and J. M. Brown, J. Chem. Phys. **99**, 3166 (1993).
[18] R. T. Carter and J. M. Brown, J. Mol. Spectrosc. **166**, 249 (1994).
[19] R. T. Carter and J. M. Brown, J. Chem. Phys. **101**, 2699 (1994).
[20] D. M. Goodridge, R. T. Carter, J. M. Brown, and T. C. Steimle, J. Chem. Phys. **106**, 4823 (1997).
[21] D. F. Hullah, R. F. Barrow, and J. M. Brown, Mol. Phys. **97**, 93 (1999).
[22] D. M. Goodridge, D. F. Hullah, and J. M. Brown, J. Chem. Phys. **108**, 428 (1998).
[23] D. F. Hullah, C. Wilson, R. F. Barrow, and J. M. Brown, J. Mol. Spectrosc. **192**, 191 (1998).
[24] C. Wilson and J. M. Brown, J. Mol. Spectrosc. **197**, 188 (1999).
[25] C. Wilson and J. M. Brown, Mol. Phys. **99**, 1549 (2001).
[26] C. Wilson, H. M. Cook, and J. M. Brown, J. Chem. Phys. **115**, 5943 (2001).
[27] W. J. Balfour, J. M. Brown, and L. Wallace, J. Chem. Phys. **121**, 7735 (2004).
[28] C. Wilson and J. M. Brown, J. Mol. Spectrosc. **209**, 192 (2001).
[29] C. W. Bauschlicher, Jr. and S. R. Langhoff, Chem. Phys. Lett. **145**, 205 (1988).
[30] S. P. Walch and C. W. Bauschlicher, Jr., J. Chem. Phys. **78**, 4597 (1983).
[31] S. R. Langhoff and C. W. Bauschlicher, Jr., J. Mol. Spectrosc. **141**, 243 (1990).
[32] D. L. Cooper, T. Thorsteinsson, and J. Garratt, Adv. Quantum Chem. **32**, 51 (1999).
[33] K. Tanaka, M. Sekiya, and M. Yoshimine, J. Chem. Phys. **115**, 4558 (2001).
[34] T. J. Sears, P. R. Bunker, A. R. W. McKellar, K. M. Evenson, D. A. Jennings, and J. M. Brown, J. Chem. Phys. **77**, 5348 (1982).
[35] S. C. Zerbetto, L. R. Zink, K. M. Evenson, and E. C. C. Vasconcellos, Int. J. Infrared Millim. Waves **17**, 1049 (1996).
[36] E. M. Telles, H. Odashima, L. R. Zink, and K. M. Evenson, J. Mol. Spectrosc. **195**, 360 (1999).
[37] E. C. C. Vasconcellos, S. C. Zerbetto, L. R. Zink, and K. M. Evenson, J. Opt. Soc. Am. B **15**, 1839 (1998).
[38] See EPAPS Document No. E-JCPSA6-124-001619 for the full version of Table II which consists of 12 pages of experimental measurements, assignments, and residuals from the least-squares fit. This document can be reached via a direct link in the online article's HTML reference section or via the EPAPS homepage (http://www.aip.org/pubservs/epaps.html).
[39] T. Nelis, S. P. Beaton, K. M. Evenson, and J. M. Brown, J. Mol. Spectrosc. **148**, 462 (1991).
[40] S. P. Beaton, K. M. Evenson, and J. M. Brown, J. Mol. Spectrosc. **164**, 395 (1994).
[41] J. M. Brown, E. A. Colbourn, J. K. G. Watson, and F. D. Wayne, J. Mol. Spectrosc. **74**, 294 (1983).
[42] J. M. Brown and A. Carrington, *Rotational Spectroscopy of Diatomic Molecules* (Cambridge University Press, Cambridge, 2003).
[43] H. E. Radford, Phys. Rev. **122**, 114 (1961).
[44] J. A. Valenti and J. M. Brown (unpublished).